IONIC CONDUCTIVITY OF $RbAg_4I_5$ IN THE MICROWAVE RANGE

by

Victor M. M. Lobo

Department of Chemistry
University of Coimbra
3000 COIMBRA - PORTUGAL

SUMMARY

The ionic conductivity σ and the complex permittivity $\hat{\varepsilon} = \varepsilon' - i\varepsilon''$ of a crystal of $RbAg_4I_5$ was calculated from measurements in the range of 27 to 39 GHz. The crystal was prepared from RbI and AgI, and tested by DC conductivity measurements. The conductivity is found to be constant in that microwave range, in contrast to what is observed in crystals such as α-AgI, α-CuI and β-CuBr, where a diffusion mechanism intermediate between the jump diffusion and the single diffusion in liquids has been proposed. Therefore, elementary steps of translational diffusion occur in a time scale faster than in the above other materials: the moving Ag^+ ion will go with less friction. The complex permittivity of $RbAg_4I_5$ has also been measured.

Key words: diffusion; jump-diffusion; ionic conductivity; permittivity; microwave technique; solid electrolytes; complex conductivity; rubidium silver iodine.

Portugaliæ Electrochimica Acta, 3 (1985) 203-222

INTRODUCTION

Measurements of the mutual isothermal diffusion coefficient D have been carried out |1| in this Department with a new open-ended capillary cell |2| which, apart from contributing to the understanding of the structure of electrolyte solutions, are urgently required by other fields of research, such as the development of the velocity correlation coefficients |3|. In fact precise measurements of D are scarce in the scientific literature as shown in |4|. However, and because our research is based on the macroscopic concept of diffusion, phenomenologically defined by Fick's first law of diffusion |5|, we felt the need to have a deeper insight to the phenomenon of diffusion itself. Consequently we attempted to study the movment of ionic species in highly conductive crystals, as is the case of $RbAg_4I_5$, using the facilities of the Physical-Chemistry Institute of the University of Göttingen, Germany.

The mechanism of self-diffusion may be pictured |6| in two extreme positions, as schematically shown in Fig. 1, representing systems of similar diffusion coefficients of the mobile particles ($D \approx 10^{-9}$ m^2 s^{-1}, the order of magnitude of those we have been measuring). On the left-hand side, we have a situation similar to that electrolyte solutions, where there is a continous type of motion obeying the laws of simple diffusion at least down to one Ångstrom and one picosecond. On the right-hand side, hydrogen in metals, like palladium and niobium, definitely performs a jump-diffusion from

Systems with $D > 10^{-5}$ cm^2 s^{-1}

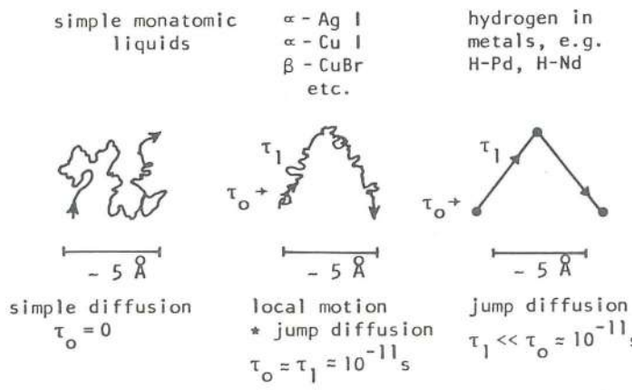

Figure 1 Diffusion in different systems.

a well defined site to another. In this case it is normally assumed that the mean time of flight τ_1, is negligible compared to the mean residence time τ_0, that is $\tau_1 << \tau_0$ where $\tau_0 \approx 10^{-11}$ seconds |7|.

The diffusion of cations in AgI-type solid electrolytes is, in a way, intermediate. Like in typical liquids there is a permanent irregular local motion. On the other hand, we also observe the resting-moving-resting kind of motion which is restricted to a three-dimensional periodic system of regions and channels defined by the addered anion lattice. Thus, there is also some resemblance to the process of jump-diffusion, constituting a solid-like aspect of the cation motion.

The idea of analysing the phenomenon of diffusion by

measurements of conductivity in crystals subject to interaction with electromagnetic radiation of large wavelength, was proposed by Prof. W. Jost, successor of Nernst as head of the Physical Chemistry Institut of Göttingen. When receiving a prize for his work, he said he had been thinking on the matter for 50 years.

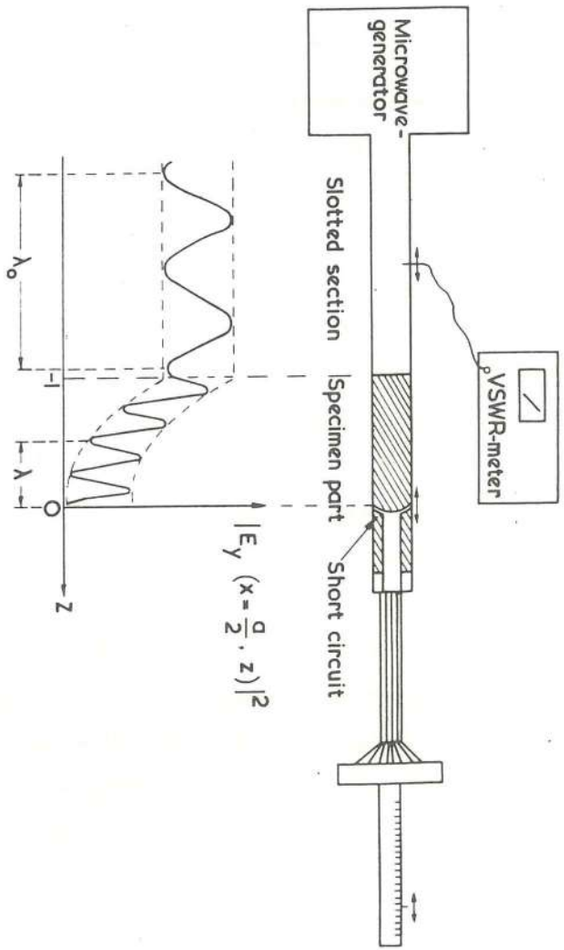

Fig. 2. Experimental arrangement and (inset) standing-wave pattern (Ref. 9).

It is now a fact that the mechanism of diffusion may be better understood by means of a technique where a sample of material such as $RbAg_4I_5$ is subject to interference with microwave radiation. The apparatus, developed by K. Funke of the same institut, Fig. 2, is capable of measuring certain parameters from which the conductivity of the sample, σ, and the complex permittivity, $\hat{\varepsilon} = \varepsilon' - i\varepsilon''$, can be computed |8, 9|.

Standing waves are used, and the radiation is within the microwave region. The two opposite side walls of a rectangular waveguide are made either of the sample to be tested (prepared by melting onto metal holders), or of silver, taken as an ideal conducting metal.

An appropriate technique allows the measurement of the wavelength λ when the radiation interacts with the sample, considered as a non-perfect conducting material (but a highly conducting one) and $\lambda_{pc} = \lambda_0$ when silver, considered as a perfect conducting material, replaces the sample. It also allows the measurement of the voltage standing wave ratio, measured in decibels, VSWRDB, as a function of a distance ℓ, the length of the material interacting with the radiation (ℓ = distance from the beginning of the specimen part to the short circuit).

The attenuation ATT(ℓ) is computed from the VSWRDB, and ideally should give a straight line, whose slope is the attenuation coefficient α. Appropriate techniques have previously been developed to calculate this α from the "sinusoidal-like" type of curve which in practice is obtained.

THEORY OF THE METHOD

The ionic conductivity in the microwave range of a crystal can be calculated from measurements performed with the equipment shown in Fig. 2, where a TE_{10}- wave(*) in a rectangular waveguide is considered, either with perfectly conducting walls (silver) or with walls of a highly conducting dielectric sample of complex permittivity $\hat{\varepsilon} = \varepsilon' - i\varepsilon''$ and conductivity $\sigma = \varepsilon_0 \varepsilon'' \omega$. The theory of the method has been described |8, 9| and we shall outline here only its main points from the above references.

Within the waveguide with perfectly conducting walls, the equation

$$\nabla^2 \hat{E} = \varepsilon_0 \mu_0 \partial^2 \hat{E} / \partial t^2 \qquad (1)$$

has to be satisfied and the TE_{10}- type solution is

$$\left.\begin{aligned} \hat{E}_x(x, z, t) &= 0 \\ \hat{E}_y(x, z, t) &= E_0 \sin(\pi x/a) \exp(j\omega t - \hat{\gamma}_{pc} z) \\ \hat{E}_z(x, z, t) &= 0. \end{aligned}\right\} \qquad (2)$$

where the symbols represent well-known parameters |e.g. 10, 11|. The propagation factor $\hat{\gamma}_{pc}$ is purely imaginary as there is no attenuation; the index pc refers to a property displayed in the waveguide with perfectly conducting walls; a is the width of the waveguide.

In the case of a waveguide with side walls of a highly

(*) TE_{10}- wave: electrical field vector in transverse to the direction of propagation of the waves; the number of standing half-waves in the x and y directions are 1 and 0, respectively.

conducting material, the TE_{10}- type solution of the wave equation is

$$\left.\begin{aligned} \hat{E}_x(x, z, t) &= 0 \\ \hat{E}_y(x, z, t) &= E_0 \sin\left(\pi \frac{x + \hat{\delta}}{a + 2\hat{\delta}}\right) \exp(j\omega t - \hat{\gamma} z) \\ \hat{E}_z(x, z, t) &= 0. \end{aligned}\right\} \qquad (3)$$

The small quantity $\hat{\delta}$ is introduced since $\hat{E}_y$ does not vanish at the walls because of the finite conductivity of the wall material. The solution of (3) is symmetric with respect to $x = a/2$. The propagation factor $\hat{\gamma} = \alpha + j\beta$ now contains an attenuation factor α and a phase coefficient β, which is generally different from the wave-number $\beta_{pc} = \hat{\gamma}_{pc}/j$. It may be also shown that

$$\hat{\delta} = \frac{\pi}{2} \frac{1}{|\hat{\gamma}^2 + (\omega/c)^2|^{1/2}} - \frac{a}{2} \qquad (4)$$

and so $\hat{\delta}$ is a function of $\hat{\gamma}$.

The imaginary part of $\hat{\delta}$ is related to the attenuation of the wave in the $\pm x$-directions, i.e. to the energy transfer into the side walls. As soon as α, ω, and $\hat{\gamma}$ are known, the field distribution $\hat{E}(r, t)$, $\hat{H}(r, t)$ within the waveguide is given by equations (3) and (4) and

$$\operatorname{curl} \hat{E} = - j\omega\mu_0 \hat{H} \qquad (5)$$

To calculate the complex permittivity we consider the field inside the specimen and then the wave equation within the dielectric, at $x \lesseqgtr 0$, may be written as

$$\frac{\partial^2}{\partial x^2}\hat{E}_y(x, z, t) = \hat{k}^2\hat{E}_y(x, z, t) \qquad (6)$$

where

$$\hat{k} = j\left[\hat{\gamma}^2 + \hat{\varepsilon}\left(\frac{\omega}{c}\right)^2\right]^{1/2} \qquad (7)$$

At the surface of the specimen, $\hat{E}_y$ has to be continuous for all possible values of z and t. Therefore the quantities $\hat{\gamma}$ and ω which describe the wave within the waveguide must also be used within the dielectric. The electric field inside the specimen, at $x \leq 0$, is

$$\left.\begin{aligned}\hat{E}_x(x, z, t) &= 0\\ \hat{E}_y(x, z, t) &= \hat{E}_y(0, z, t)\exp(\hat{k}x)\\ \hat{E}_z(x, z, t) &= 0\end{aligned}\right\} \qquad (8)$$

With the help of equation (5) the magnetic field inside the specimen is obtained. The requirement that $\hat{H}$ be continuous at the surface of the specimen leads to an expression for $\hat{k}$. Equating $\hat{H}_z(0, z, t)$ derived from (3), (5) and (8) gives

$$\hat{k} = \left(\frac{\pi}{a + 2\hat{\delta}}\right)\cdot\cot\left(\frac{\pi\hat{\delta}}{a + 2\hat{\delta}}\right) \qquad (9)$$

and the complex permittivity may be calculated from equation (7):

$$\hat{\varepsilon} = -\left(\frac{c}{\omega}\right)^2(\hat{k}^2 + \hat{\gamma}^2) \qquad (10)$$

Thus, when a, ω, and $\hat{\gamma}$ are known, $\hat{\varepsilon}$ can be calculated.

EXPERIMENTAL AND CONCLUSIONS

The structure of $RbAg_4I_5$ had been described by Geller |12|. For the present work, a sample of $RbAg_4I_5$ crystal was prepared by fusing at 750°C in a vacuum line, with a low pressure of N_2 (about 1/3 atm.), a mixture of 1 part of RbI to 4 parts of AgI. The powder, finely divided and thouroughly mixed for a few hours, is carefully placed in a quartz ampoule, heated in darkness up to around 725°C above room temperature (29 mV on the thermocouple reading) for 30 minuts. Eventually the ampoule is sealed with acetylene/oxygene flame. Once fused, the sample must be cooled as fast as possible, and so it is dropped in cold water. The crystal is then carefully polished.

A quality control test is carried out by measuring its DC conductivity applying the van der Paw method |13|. Four silver electrodes, A, B, C, D, Fig. 3, were soldered to a rectangular crystal with both faces polished with sand paper, using an H_2/O_2 flame. A 400 Hz signal is applied to A and B

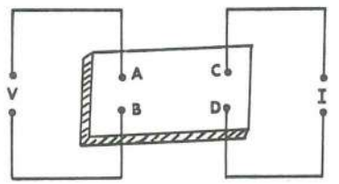

Fig. 3. Measurement of the DC conductivity σ_0 by the van der Paw method.

and simultaneously the current flowing between C and D is read. This procedure is repeated with points A + C and B + D. From the results of a particular case, the DC conductivity was calculated to be 0.199 $(\Omega cm)^{-1}$, a value close enough to the expected 0.165 and so the crystal can be considered of good enough quality. Similar results were obtained with other samples. Whereas $\sigma(RbAg_4I_5) \simeq 0.2$ $(ohm\ cm)^{-1}$, we should see that $\sigma(NaCl) \simeq 10^{-8}$ and $\sigma(Ag) \simeq 10^{5}$.

A few samples of $RbAg_4I_5$ crystals were made and the best ones choosen for microwave tests.

The microwave apparatus used, Fig. 2, has been previously described [9] and consists basically of a Hewlett Packard HP8090A Sweep Oscillator, a HP 415 SWR meter and an appropriately designed compartment to hold the cell with the $RbAg_4I_5$ crystal.

The microwave generator may be set at desired frequencies. We have choosen to work at frequencies 27.01_0, 29.00_0, 31.00_0, 33.00_0, 35.00_2, 37.00_0 and 38.53_2 GHz, after some preliminary trials. The short circuit represented in Fig. 2 can be moved within the waveguide and its location can be determined with an uncertainty of ± 0.01 mm. Fig. 4 shows the results taken when we moved the short circuit from 90 to 50 mm by steps of 1 mm. The wavelength has been measured with the walls of the waveguide made up of pure silver, and made up of $RbAg_4I_5$ sample, at everyone of the above frequencies (Table I).

The attenuation parameter ATT(ℓ), shown in table II is calculated from VSWR DB readings for every position of the short circuit from 90 to 50 mm in 1 mm steps, and from it, all the

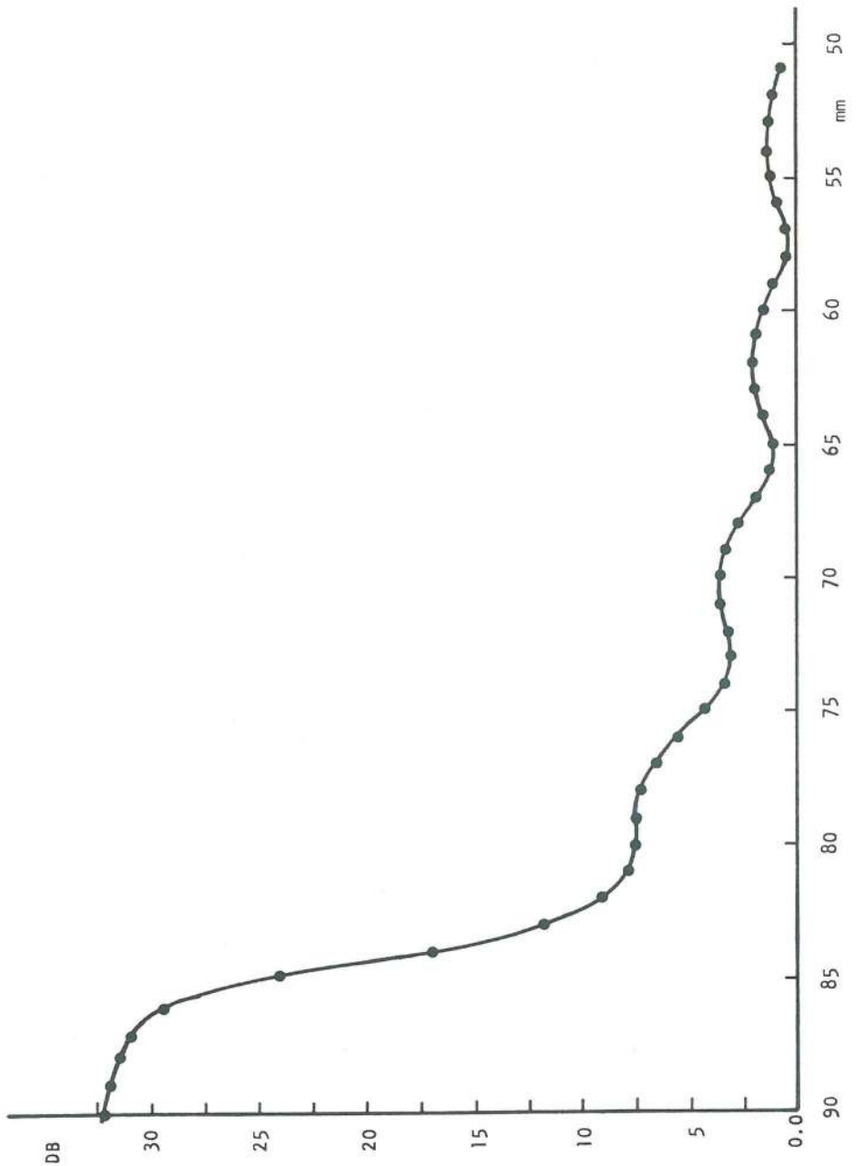

Fig. 4. Readings of the voltage standing wave ratio in decibels (VSWRDB) versus distance of the short circuit (Fig. 1), from 90 to 50 mm in steps of 1 mm, at 27.010 GHz.

other parameters of table II were calculating using a programmable calculator, according to complex equations previously described |8|. Ideally a plot of ATT(ℓ) versus ℓ/mm should be a straight line, and α its slope, but Fig. 5 shows a practical case at one of the frequencies (27.01_0 GHz) and α is calculated by graphical readings.

TABLE I

1/2 wavelength in the case of pure silver walls (Fig. 2) in the waveguide (blank) and in the case of $RbAg_4I_5$ wall with thickness of 1.55 mm (or 1.00 mm denoted by *).

Frequency/GHz		1/2 wavelength/mm	
Blank	$PbAg_4I_5$	Blank	$RbAg_4I_5$
27.01o	27.00_8	8.75_2	8.16_{95}
(29.00o)	29.00o		7.08_{18}
31.00o	31.00o	6.52_6	6.29_{86}
(33.00o)	33.00o		5.45_{15}
35.00_2	35.00_2	5.32_4	5.22_{72}
(37.00o)	37.00o		4.82_{13}
38.53_2	38.53_2	4.62_6	4.55_{42}
27.01o*	27.01o*		8.39_{96}
31.00o*	31.00o*		6.34_{95}

TABLE II

Attenuation factor ATT(1) calculated from voltage standing wave ratios in decibels (VSWR DB) measured at specified frequencies as the short circuit of Fig. 2 is moved from 90 to 50 mm by steps of 1 mm.

Freq. \ mm	VSWR & ATT	90	89	88	87	86	85	84	83
29.000	VSWR	33.1	32.9	32.2	31.4	28.15	20.55	15.36	11.31
	ATT	*0.022*	*0.023*	*0.025*	*0.027*	*0.039*	*0.094*	*0.172*	*0.279*
31.000	VSWR	34.6	34.0	33.2	32.1	28.5	21.45	15.43	11.97
	ATT	*0.019*	*0.020*	*0.022*	*0.025*	*0.038*	*0.085*	*0.171*	*0.258*
33.000	VSWR	35.3	34.5	33.4	31.45	27.13	20.72	15.65	13.15
	ATT	*0.017*	*0.019*	*0.021*	*0.027*	*0.044*	*0.092*	*0.167*	*0.224*
35.002	VSWR	34.6	33.0	32.1	31.4	27.18	20.45	15.75	13.85
	ATT	*0.019*	*0.022*	*0.025*	*0.027*	*0.044*	*0.095*	*0.165*	*0.206*
37.000	VSWR	34.5	32.9	31.9	31.2	26.42	19.70	15.56	14.29
	ATT	*0.019*	*0.023*	*0.025*	*0.028*	*0.048*	*0.104*	*0.168*	*0.195*
38.532	VSWR	33.4	33.1	31.45	30.6	24.75	18.13	14.85	14.05
	ATT	*0.0214*	*0.0221*	*0.0268*	*0.0295*	*0.0579*	*0.125*	*0.183*	*0.201*

Freq. \ mm	VSWR & ATT	82	81	80	79	78	77	76	75
29.000	VSWR	9.05	7.80	8.30	8.27	7.63	6.40	5.18	4.36
	ATT	*0.365*	*0.407*	*0.405*	*0.409*	*0.442*	*0.521*	*0.620*	*0.702*
31.000	VSWR	10.74	10.58	10.60	9.78	8.65	6.70	6.00	6.05
	ATT	*0.299*	*0.305*	*0.304*	*0.336*	*0.388*	*0.500*	*0.551*	*0.547*
33.000	VSWR	12.50	12.55	11.78	10.08	8.56	7.93	7.00	6.97
	ATT	*0.242*	*0.240*	*0.264*	*0.324*	*0.392*	*0.425*	*0.481*	*0.482*
35.002	VSWR	13.55	13.48	12.03	10.08	9.30	9.15	9.13	8.44
	ATT	*0.213*	*0.215*	*0.256*	*0.324*	*0.357*	*0.364*	*0.365*	*0.398*
37.000	VSWR	14.37	13.65	11.83	10.35	9.94	9.91	9.50	8.38
	ATT	*0.194*	*0.211*	*0.262*	*0.314*	*0.330*	*0.331*	*0.348*	*0.401*
38.532	VSWR	14.00	12.85	10.90	10.10	10.06	9.82	8.80	7.90
	ATT	*0.202*	*0.232*	*0.293*	*0.323*	*0.325*	*0.335*	*0.380*	*0.427*

Freq. \ mm		74	73	72	71	70	69	68	67
29.000	VSWR	4.17	4.35	4.44	4.16	3.46	2.74	2.27	2.16
	ATT	*0.723*	*0.703*	*0.693*	*0.725*	*0.813*	*0.927*	*1.020*	*1.045*
31.000	VSWR	6.35	6.10	5.20	4.15	3.68	3.75	4.13	4.12
	ATT	*0.525*	*0.543*	*0.618*	*0.725*	*0.783*	*0.774*	*0.728*	*0.729*
33.000	VSWR	7.29	6.14	5.38	5.35	5.56	5.46	4.74	3.93
	ATT	*0.462*	*0.540*	*0.602*	*0.604*	*0.986*	*0.595*	*0.662*	*0.752*
35.002	VSWR	7.33	6.62	6.62	6.60	6.24	5.49	4.94	4.84
	ATT	*0.460*	*0.506*	*0.506*	*0.507*	*0.533*	*0.592*	*0.642*	*0.652*
37.000	VSWR	7.62	7.51	7.50	6.93	6.22	5.60	5.81	5.82
	ATT	*0.442*	*0.449*	*0.490*	*0.481*	*0.534*	*0.967*	*0.563*	*0.565*
38.532	VSWR	7.65	7.61	7.26	6.49	6.03	6.01	5.96	5.49
	ATT	*0.441*	*0.440*	*0.464*	*0.515*	*0.549*	*0.550*	*0.554*	*0.592*

Freq. \ mm		66	65	64	63	62	61	60	59
29.000	VSWR	2.49	2.67	2.55	2.10	1.53	1.08	1.15	1.45
	ATT	*0.975*	*0.940*	*0.965*	*1.059*	*1.216*	*1.390*	*1.358*	*1.243*
31.000	VSWR	3.63	2.70	2.13	2.25	2.70	2.91	2.55	1.95
	ATT	*0.790*	*0.935*	*1.052*	*1.025*	*0.935*	*0.898*	*0.963*	*1.096*
33.000	VSWR	3.56	3.78	3.99	3.78	3.12	2.50	2.48	2.8
	ATT	*0.799*	*0.770*	*0.744*	*0.770*	*0.864*	*0.973*	*0.977*	*0.917*
35.002	VSWR	4.95	4.73	4.28	3.65	3.60	3.78	3.70	3.23
	ATT	*0.641*	*0.663*	*0.710*	*0.787*	*0.794*	*0.770*	*0.781*	*0.847*
37.000	VSWR	5.30	4.75	4.52	4.56	4.50	4.06	3.65	3.56
	ATT	*0.609*	*0.661*	*0.684*	*0.680*	*0.684*	*0.736*	*0.787*	*0.799*
38.532	VSWR	4.90	4.82	4.83	4.65	4.17	3.90	3.97	3.90
	ATT	*0.646*	*0.654*	*0.653*	*0.671*	*0.723*	*0.755*	*0.747*	*0.755*

Freq. \ mm		58	57	56	55	54	53	52	51
29.000	VSWR	1.70	1.67	1.40	0.92	0.45	0.55	0.92	1.18
	ATT	*1.164*	*1.173*	*1.260*	*1.470*	*1.827*	*1.727*	*1.470*	*1.345*
31.000	VSWR	1.28	1.26	1.73	2.05	1.97	1.49	0.80	0.58
	ATT	*1.305*	*1.313*	*1.155*	*1.071*	*1.091*	*1.229*	*1.539*	*1.700*
33.000	VSWR	2.96	2.62	2.00	1.58	1.78	2.14	2.19	1.80
	ATT	*0.890*	*0.950*	*1.083*	*1.200*	*1.141*	*1.050*	*1.038*	*1.153*
35.002	VSWR	2.75	2.68	2.87	2.90	2.55	2.08	1.89	2.13
	ATT	*0.926*	*0.938*	*0.905*	*0.900*	*0.963*	*1.064*	*1.111*	*1.052*
37.000	VSWR	3.67	3.59	3.13	2.80	2.82	2.99	2.77	2.36
	ATT	*0.785*	*0.802*	*0.855*	*0.917*	*0.913*	*0.893*	*0.922*	*1.001*
38.532	VSWR	3.60	3.27	3.14	3.25	3.12	2.76	2.54	2.58
	ATT	*0.794*	*0.841*	*0.861*	*0.844*	*0.864*	*0.924*	*0.965*	*0.957*

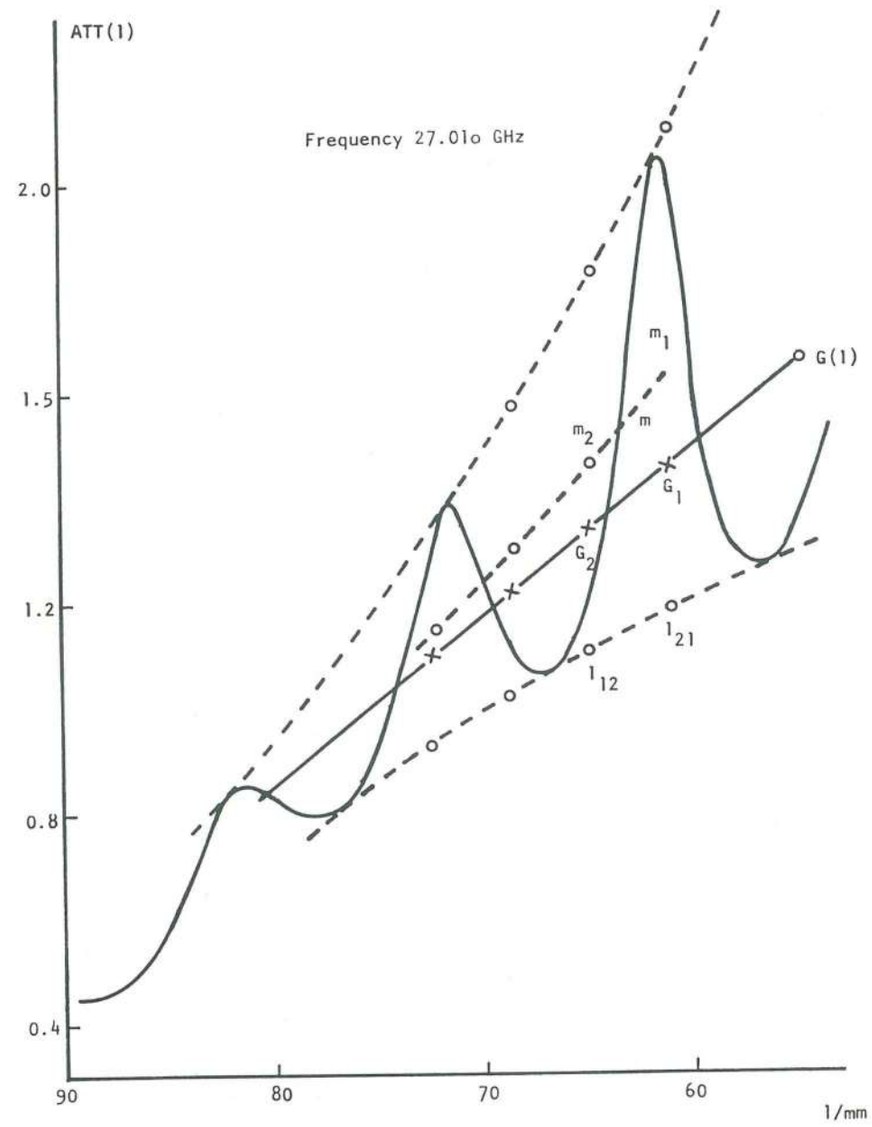

Fig. 5. Plot of ATT(ℓ) versus the distance ℓ/mm of the short circuit (Fig. 1) for the calculation of the attenuation coefficient α at one of the working frequencies (27.010 GHz). In this case, $\alpha = \frac{1.66-1.18}{6.4-5.2} = 0.40_0 cm^{-1}$.

TABLE III

Summary of results from microwave interaction with a $RbAg_4I_5$ sample at specified frequencies.

Frequency ν	λ_0	λ	a	α	δ = g+hi	ξ = r+is	x = u+iω	ε'	ε''	σ
27.01_0	1.7504	1.6339	0.718	0.40	0.013215-0.032618i	$8.3668x10^{-2}$-.21004i	1.5991+4.4819i	13.831	11.144	0.217
31.00_0	1.3052	1.25972	0.720	0.307	0.011991-0.032439i	$7.5887x10^{-2}$-.20875i	1.5940+4.6143i	19.077	14.578	0.251
35.00_2	1.0648	1.04544	0.721	0.263	0.0079740-0.032531i	$5.0316x10^{-2}$-.20896i	1.4444+4.9366i	17.906	11.089	0.216
38.53_2	0.9252	0.9108_4		0.219	0.0101-0.0314i	$6.410x10^{-2}$-.2017i	1.6275+4.826$_7$i	13.9_1	10.07	0.216

ν = frequency, set at desired values; λ_0, λ = wavelengs in blank and in $RbAg_4I_5$ measured experimentally;

a = width of the wave-guide; α = attenuation factor calculated from

$$G(1) = \overline{ATT}(1) - \frac{1}{2}\ln\{\cos h\,(\Delta\overline{ATT}(1))\} = \alpha\,1 + \varepsilon/2;$$

$$\delta = g + hi = \frac{\pi}{2}\{\alpha^2 - (\frac{2\pi}{\lambda})^2 + (\frac{2\pi}{\lambda_0})^2 + (\frac{\pi}{a})^2 + \frac{4\pi\alpha}{\lambda}\,i\}^{-1/2} - \frac{a}{2} \qquad \xi = r + is = \frac{1}{\text{thickness}}\ tg\,(\frac{\pi\delta}{a+2\delta})\,(\frac{a+2\delta}{\pi})\ \xi = f(\hat{\kappa})$$

$$\xi = \frac{tg^2 x}{x} \quad \text{where } x = \mu + i\omega$$

$$\hat{\varepsilon} = -(\frac{c}{\omega})^2\{(\frac{x}{\text{thickness}})^2 + \alpha^2 - \frac{4\pi^2}{\lambda^2} + \frac{4\pi\alpha}{\lambda}\,i\} = \varepsilon' - i\varepsilon'' \qquad \sigma = \varepsilon_0\varepsilon''\omega \qquad (\hat{\sigma} = i\varepsilon_0\hat{\varepsilon}\omega)$$

A summary of the results is shown in table III.

The main conclusion we may derive from the above measuments on the $RbAg_4I_5$ samples we have prepared, is that the conductivity σ is constant over the whole range 27 - 39 GHz. In fact, from table III we see that σ is about 0.22 ohm^{-1} cm^{-1} for all the studied frequencies except one where we obtained the slightly higher value of 0.25 ohm^{-1} cm^{-1}. The results are in very good agreement with those of Scrosati, Germano and Pistoia |14| who, using a rather different method, obtained values from 0.20 to 0.24 ohm^{-1} cm^{-1}. These authors also discuss measurements previously published |15 – 20| which are considerable divergent. Later in the same year, Sacrosati |21| found a lower value of 0.1 ohm^{-1} cm^{-1} for $RbAg_4I_5$ crystallized from an acetone solution.

Therefore elementary steps of translational diffusion occur in a time scale faster than in other materials previously studied by K. Funke and others from the W. Jost school, namely α-AgI |22|, α-CuI |23| and β-CuBr |24|.

The time the ions are in motion is shorter than an upper limit, say less than about 5 pico-seconds: $\tau < 5$ ps. More than half of the ions are on flight in the previously studied α-AgI, whereas in the present sample, $RbAg_4I_5$, because of the low value of the DC conductivity, one would predict that the residence time τ_0 is smaller than the flight time τ_1. Therefore we may conclude that the moving Ag^+ ion will go with less friction in the present case than in previously studied cases.

Another feature of the present work is the computation of the complex permittivity, $\hat{\varepsilon} = \varepsilon' - i\varepsilon''$, of the $RbAg_4I_5$ crys-

tal. We observe that ε' is also constant and it is positive in contrast with other substances such as α-AgI.

ACKNOWLEDGEMENTS: We are thankful to DAAD (Deutscher Akademischer Austauschdienst) for a 2 month grant to Germany, to INIC for financial support to our research project, to Professors W. Jost and K. Funke for their kind assistance in this work, and to Prof. Margarida Ramalho Costa for her kind help in assisting the author in matters concerning the propagation of the electromagnetic field.

REFERENCES

| 1| V. M. M. Lobo and M. H. Teixeira, *Electrochimica Acta 24, 565 (1979);* V. M. M. Lobo and M. H. Teixeira, *Electrochimica Acta 27, 1145 (1982);* V. M. M. Lobo and L. C. Gonçalves, *Electrochimica Acta 27, 1343 (1982)*; V. M. M. Lobo and M. H. Teixeira, *Electrochimica Acta 27, 1509 (1982)*; V. M. M. Lobo and J. L. Quaresma, *communication to the 6th Meeting of the Port. Chem. Soc., Aveiro (1983)*; V. M. M. Lobo and J. L. Quaresma, *communication to the 7th Meeting of the Port. Chem. Soc., Lisbon (1984).*

| 2| V. M. M. Lobo, *Ph. D. Thesis, Cambridge (1971)*; J. N. Agar and V. M. M. Lobo, *J. Chem. Soc., Faraday Trans. I, 71, 1659 (1975).*

| 3| H. G. Hertz and R. Mills, *J. Phys. Chem. 82, 952 (1978).*

| 4| V. M. M. Lobo, *Electrolyte Solutions: Literature Data on Thermodynamic and Transport Properties, Coimbra (1975), and Vol. II of the same work, recently published (1984).*

| 5| A. Fick, *Pogg. Ann. 94, 59 (1855).*

| 6| C. Clemen and K. Funke, *Ber. Bunsen-Ges. phys. Chem. 79, 1119 (1975).*

| 7| K. Funke, *Semiconductors and Insulators 3 (4), 351 (1978).*

| 8| K. Funke, *Untersuchungen der Komplexen Dielektrizitätskonstante des α-Silberjodids im Mikrowellengebiet und im Fernen Infrarot – Dissertation, Göttingen (1970).*

| 9| K. Funke, *Proc. Conf. Meas. High Freq. Die. Prop. Mat., London (1972).*

|10| M. Silva, *Teoria do Campo Electromagnético, Coimbra (1945).*

|11| B. G. Levich, *Theoretical Physics, Vol. II, North-Holl and Publ. Comp., London (1971).*

|12| S. Geller, *Science 157, 310 (1967).*

|13| V. Paw, *Phillips Res. Rep. 13, 1 (1958).*

|14| B. Scrosati; G. Germano and G. Pistoia, *J. Electrochem. Soc. 118, 86 (1971).*

|15| J. N. Bradley and P. D. Greene, *Trans. Faraday Soc. 63, 424 (1967).*

|16| B. B. Owens and G. R. Argue, *Science 157, 308 (1967).*

|17| T. Takahashi and O. Yamamoto, *J. Electrochem. Soc. 117, 1 (1970).*

|18| M. De Rossi; G. Pistoia and B. Scrosati, *J. Electrochem. Soc. 116, 1964 (1969).*

|19| J. E. Oxlev and J. R. Humphrey, *Atomics Int., Final Report, July 22 - Oct. 22 (1968).*

|20| L. D. Fullmer and M. A. Hiller, *J. Crystal Growth, 5, 395 (1969).*

|21| B. Scrosati, *J. Electrochem. Soc. 118, 899 (1971).*

|22| K. Funke and A. Jost, *Ber. Bunsen-Ges. phys. Chem. 75, 436 (1971).*

|23| K. Funke and R. Hackenberg, *Ber. Bunsen-Ges. phys. Chem. 76, 885 (1972).*

|24| C. Clemen, *Messung der komplexen Dielektrizitätsfunktion von β-Kupfer(I)-Bromid im Wikrowellengebiet – Dissertation, Göttingen (1975).*

(Received 16 January 1985
In revised form 25 October 1985)

CINÉTICA DE DISSOLUÇÃO DE UM AÇO INOXIDÁVEL EM SOLUÇÕES CONCENTRADAS DE CLORETO

Mário Barbosa

Departamento de Engenharia Metalúrgica
Faculdade de Engenharia
Universidade do Porto
4099 PORTO CODEX
PORTUGAL

This paper describes results obtained with an AISI 304 stainless steel in 1 M HCl and 1 M KCl solutions, with the aim of contributing to the understanding of the processes occurring within growing pits. The kinetics of dissolution were studied at constant potential by the scratch method. In 1 M HCl a salt film formed below the passivation peak and its rate of formation increased as the applied potential was made more noble. In 1 M KCl the rate of film formation was not affected by potential. In this solution a passivating film developed even before the current maximum in the anodic polarization curve. Since the solutions found within growing pits usually have low pH and high chloride concentrations it is concluded that, as pits develop, their surface should become covered by salts layers of increasing thickness.

Key Words: dissolution kinetics, pitting, stainless steel

INTRODUÇÃO

É bem conhecido o facto de existirem altas concentrações de cloretos e de hidrogeniões nas picadas que se formam em vários metais, nomeadamente nos aços inoxidáveis. Estas concentrações são responsáveis pela elevada ve-